Impacts of mesoscale processes on biogeochemical fluxes in the North Atlantic: a basin-scale eddy-resolving (0.1°) simulation

The POP-BGC Group

February 16, 2001

Draft Manuscript

Abstract

1. Introduction

The fact that geochemical estimates of new production in the oligotrophic waters of the open ocean far surpass that which can be sustained by traditional mechanisms of nutrient supply has been problematic for some time (Shulenberger and Reid, 1981; Jenkins and Goldman, 1985). Three independent transient tracer techniques all indicate that new production in the Sargasso Sea is on the order of 0.5 mol N m^{-2} yr^{-1}: oxygen production in the euphotic zone (Jenkins and Goldman, 1985; Spitzer and Jenkins, 1989), oxygen consumption in the aphotic zone (Jenkins and Goldman, 1985; Sarmiento *et al.*, 1990; Jenkins and Wallace, 1992), and the Helium flux gauge (Jenkins, 1988a). Approximately one quarter to one third of the annual nutrient requirement can be supplied by entrainment into the surface mixed layer caused by wintertime convection (Michaels *et al.*, 1994). Modern estimates of mixing rates in the thermocline (Lewis *et al.*, 1986; Ledwell *et al.*, 1993; Ledwell *et al.*, 1997) combined with the observed nutrient gradient at the base of the euphotic zone suggest that diapycnal diffusion contributes very little. Wind-driven vertical motion in the main subtropical gyre is oriented downward due to the negative wind stress curl in the region and therefore represents a net sink rather than a net source of nutrients. The surface Ekman drift does advect nutrients horizontally toward the interior of the gyre, but recent calculations suggest the net contribution of the wind driven transport is small and positive (Williams and Follows, 1997). Together these processes account for less than one half the annual nutrient budget. It has been suggested that nitrogen fixation could be responsible for the remainder of the phytoplankton nutritional requirement, yet rate estimates for this region vary by an order of magnitude (Michaels *et al.*, 1996; Lipschultz and Owens, 1996; Capone *et al.*, 1997; Gruber and Sarmiento, 1997; also see the review by Hood *et al.*, 2000).

[SCD comment: need a statement about DOM advection a la Rintoul and Wunsch]

The notion that mesoscale processes could be an important vehicle for nutrient transport in the world's oceans has been debated for many years (*e.g.* Woods, 1988; Fasham *et al.*, 1985; Franks *et al.*, 1986; Falkowski *et al.*, 1991; Strass, 1992; Flierl and Davis, 1993; Dadou *et al.*, 1996; Smith *et al.*, 1996; Spall and Richards, 2000; Mahadevan and Archer, 2000; Garcon *et al.*, in press). Comparison of two hydrographic profiles sampled one month apart in the summer of 1986 off Bermuda documented an apparently eddy-driven nutrient injection event that could account for 20-30% of the annual new production (Jenkins, 1988b). In the decade that has passed since those observations were first published, substantial evidence has accumulated that mesoscale eddies are a significant mode of nutrient transport in the Sargasso Sea (McGillicuddy *et al.*, 1998). High resolution regional numerical simulations in this area suggest eddy-induced upwelling causes intermittent fluxes of nitrate into the euphotic zone of magnitude sufficient to balance the nutrient demand implied by geochemical estimates of new production (McGillicuddy and Robinson, 1997). Nitrate flux calculations based on satellite altimetry and a statistical model linking sea level anomaly to subsurface isopycnal displacements provide estimates of comparable order (Siegel *et al.*, 1999). Observations of a nutrient pulse associated with a mesoscale eddy were obtained using novel chemical sensing technology deployed on the Bermuda Testbed Mooring (McNeil *et al.*, 1999). Mesoscale biogeochemical surveys carried out as part of the BATS Validation activities have documented the impact of mid-ocean eddies on nutrient and biomass distributions. These observations demonstrate that eddy-induced upward displacement of density surfaces can inject nutrients into the euphotic zone which results in the accumulation of phytoplankton biomass in the overlying waters (McGillicuddy *et al.*, 1999). Similar patterns emerge from an analysis of satellite-derived sea-surface temperature and pigment fields (McGillicuddy *et al.*, in press). Analysis of the 21 instances during the lifetime of the Coastal Zone Color

Scanner (CZCS) in which simultaneous AVHRR and ocean color images are available show that higher (lower) pigment biomass occurs in mesoscale features consisting of cold (warm) temperature anomalies.

Until recently, computational limitations precluded the treatment of mesoscale processes in basin-scale biogeochemical modeling studies. The seminal work of Sarmiento *et al.* (1993) and Fasham *et al.* (1993) documented the first substantial effort to use a planktonic ecosystem model embedded in a general circulation model (GCM) to investigate the physical-biological interactions which impact biogeochemical budgets in the North Atlantic. Their general approach was to incorporate Fasham *et al.*'s (1990) seven compartment nitrogen-based biological formulation into a relatively coarse resolution (2°) primitive equation circulation model. Under seasonal climatological forcing conditions, the coupled model was run out to a quasi-steady statistical equilibrium and the underlying controls were diagnosed. Subsequent work has included a parameter dependence and sensitivity analysis of these numerical solutions conducted by Slater *et al.* (1993), and some initial experiments involving assimilation of satellite-derived chlorophyll distributions (Armstrong *et al.*, 1995). Oschlies and Garcon (1998, 1999) and Oschlies *et al.* (2000) used a simpler four-compartment NPZD ecosystem model in an eddy-permitting (1/3 °) resolution model of the North Atlantic. Dutkiewicz *et al.* (in press) examine interannual variations in basin-scale chlorophyll patterns using a simple ecosystem model in a coarse resolution GCM.

Detailed comparisons of these simulations to observations has revealed mixed results. One aspect in which the model solutions agree with data is the large scale chlorophyll distribution (Sarmiento *et al.*, 1993; Oschlies *et al.*, 2000). The overall pattern in the annual mean concentration is similar to satellite-based estimates from CZCS, including low pigment in the main subtropical gyres, and higher concentrations in upwelling regions and the subpolar

gyre. Furthermore, the modeled seasonal variations about the annual mean also compare favorably with observations. Given the fact that such simulations were constructed using a fixed set of ecosystem parameters over the entire domain, this agreement is especially intriguing.

Although such models capture the general characteristics of the seasonal changes in surface chlorophyll, comparison with time series data at fixed points reveals significant problems. For example, wintertime nitrate concentrations at Station S exceed observed values by up to an order of magnitude (Fasham *et al.*, 1993; Oschlies *et al.*, 2000). The vertical structure of the simulated distribution is also suspect, in that the nitracline is much shallower and sharper than is observed. Simulated phytoplankton concentration and primary production tend to have seasonal cycles of much higher amplitude than what is observed. These systematic errors tend to compensate for each other in terms of annual primary production, producing the "right" answer for the "wrong" reasons: over(under)estimation during the bloom(oligotrophic) periods.

[SCD suggests highlighting other deficiencies of these solutions: too low spring bloom in temperate/subpolar gyre (lack of second size class?); way too low biomass and productivity in southern half of subtropical gyre (all the way across not just Sargasso Sea) (mesoscale eddies, N2 fixation?, microbial loop)]

Analysis of the annual nutrient budgets near Bermuda (Table 1) reveals even more troublesome issues. In the Fasham *et al.* (1993) analysis, nitrate supply is dominated by horizontal advection, mostly in the meridional direction. Convection is the next largest contribution to the annual budget, but nearly one half of the convective input is counterbalanced by downwelling driven by Ekman convergence (the vertical advection term). Diffusion plays only a minor role, and the balance of terms yields an annual new production which is within

the range of geochemical estimates (0.50 ± 0.14 mol N m^{-2} yr^{-1}). In contrast, the eddy-permitting simulation of Oschlies *et al.* (2000) suggests far less lateral input of nitrate in this region. The annual new production of 0.66 mol N m^{-2} yr^{-1} is at the upper limit of observational estimates, and is almost entirely driven by vertical mixing (Oschlies *et al.* do not distinguish between convection and diffusion in their model). Interestingly, both the coarse resolution and eddy permitting simulations predict similar fluxes due to vertical advection (net transport out of the euphotic zone). Both are forced with monthly climatological winds described by Hellerman and Rosenstein (1983), so the Ekman downwelling driven by wind stress curl is likely comparable in the two models. If the bulk fluxes of nitrate are not sensitive to differences in either (1) the biogeochemical models, or (2) the simulated nitrate fields on which the transport processes operate, it could be inferred that eddy activity in the Oschlies *et al.* eddy-permitting model does not contribute significantly to new production near Bermuda. Here we present a high-resolution (0.1°) eddy resolving simulation of the North Atlantic which suggests that vertical transport associated with mesoscale features is sufficiently strong to overcome Ekman downwelling in the subtropical gyre, causing vertical advection to be a net source of nitrate in this region.

Methods

Physical model

The coupled physical-biogeochemical model is based on the Los Alamos Parallel Ocean Program (POP) (Smith *et al.*, 1992). It is a level-coordinate model that solves the three-dimensional primitive equations with a free surface and realistic bottom topography. Essentially it is an implementation of primitive equation ocean dynamics described in Bryan (1969), with a number of important numerical improvements. In addition, it has been

adapted to run efficiently on massively parallel computational architectures.

The model domain extends from 20°S in the South Atlantic to 72.6°N in the North Atlantic, and from 98°W to 17.2°E (Figure 1). It includes the Gulf of Mexico and the western Mediterranean Sea, but excludes Hudson Bay. The computational mesh consists of a Mercator grid with a resolution of $\Delta\lambda = 0.1°$ and $\Delta\phi = 0.1°\cos\phi$ where λ and ϕ are longitude and latitude, respectively. The horizontal resolution varies from 11.1km at the equator to 3.2km at the northern boundary, such that the grid spacing is everywhere less than or equal to the zonal-mean Rossby radius of deformation. The vertical grid consists of 40 non-uniformly spaced levels, distributed in a Gaussian function of depth. Level thicknesses vary from approximately 10m at the surface to 250m at mid-depth. Bathymetry was derived from the $\frac{1}{12}^\circ$ resolution ETOPO5 database from the National Geophysical Data center.

Subgridscale horizontal mixing processes are parameterized with a biharmonic operator. Viscosity and diffusivity vary with the cube of the grid spacing, using values that are as small as possible yet still maintain computational stability. Vertical viscosities and diffusivities are computed based on the Richardson number formulation described by Pacanowski and Philander (1981) with background values of 10^{-4} and 10^{-5} m^2 s^{-1}, respectively. In addition to this explicit integration of the vertical mixing terms, two passes of a standard convective adjustment scheme are made each time step. A quadratic bottom stress is applied at the ocean bottom.

The model ocean is initialized at rest, with temperature and salinity values set to their climatological values for June in the Levitus (1982) climatology. Surface forcing consists of six-hourly ECMWF surface wind analyses averaged over daily intervals, with surface heat fluxes derived from the Barnier *et al.* (1995) monthly climatology. Freshwater fluxes are simulated by restoring surface salinity to daily interpolations of the Levitus (1982) monthly

climatology. There are 3°-wide buffer zones at the northern, eastern and southern boundaries in which temperature and salinity are also restored to the Levitus climatology; the restoring time scale varies linearly from zero at the boundary to 15 days at the edge of the buffer.

The physical model is spun up for a period of 11.5 years using repeating winds from 1985-1991. During this time, the model reaches a state of quasi-equilibrium. Kinetic energy reaches stationarity in 2-3 years, which is a typical time scale for baroclinic adjustment of the velocity field to an initial density distribution. Volume-averaged temperature approaches a steady annual cycle after approximately ten years. Although these integrated statistics suggest that the initial phase of rapid adjustment to initial conditions is complete, there is a much longer time scale (on the order of the turnover time for the entire basin) for the model to achieve true equilibrium. Current computational capabilities do not permit integrations of such duration.

See Smith *et al.* (2000) for a detailed description of the 0.1° simulation on which the coupled model is based.

An idealized nutrient transport model

In order to ascertain the impact of various circulation processes on nutrient transport to the upper ocean, an idealized one-tracer model representing nitrate was incorporated into the physical model described above. In this model, the water column is partitioned into a euphotic zone (above 104m) where biological uptake of nitrate occurs and an aphotic zone (below 104m) where nitrate is restored to its observed concentration as a spatial function of density via a first-order reaction. Nitrate uptake by phytoplankton is assumed to take the form

$$\text{uptake rate} = \mu \min(Q, L)$$

where the temperature-dependent maximal uptake rate μ is modulated by non-dimensional light and nutrient limitation factors via Liebig's Law of the Minimum (Liebig, 1845; Kiefer and Mitchell, 1983; Hurtt and Armstrong, 1996). Nutrient limitation Q is expressed in Michaelis-Menten form, whereas light limitation is formulated as an exponential function characteristic of traditional photosynthesis versus irradiance relationships (*e.g.* Platt *et al.*, 1980), although effects of photoinhibition are neglected:

$$Q = N/(k_n + N) \qquad L = 1 - \exp(-\alpha I)$$

The temperature dependence of the maximal rate is given by Eppley's (1972) formula $\mu = \mu_0 1.884^{(T-20)/10}$. Photosynthetically available radiation (I) is assumed to be 45% of the shortwave flux specified in the Barnier *et al.* (1995) monthly climatology. A constant extinction coefficient of 0.044 m^{-1} is used to compute the underwater light field. The impact of mixing on primary production in the surface layer is modeled by subjecting the entire mixed layer to a light intensity that is averaged over that depth interval. See Table 2 for a list of model parameter definitions and values.

Remineralization of nitrate in the aphotic zone is parameterized as a first-order relaxation to observations with time scale τ:

$$\text{remineralization rate} = \tau(NO_3^*(i, j, \sigma_\theta^*) - NO_3)$$

where $NO_3^*(i, j, \sigma_\theta)$ is interpolated from a three-dimensional lookup table in which every (i, j) grid point in the model has a nitrate–density relationship based on the nitrate field from the NODC World Ocean Atlas 1998 (WOA98). The reference density field σ_θ^* is an average of the simulated density from the final two years of the spinup period. Use of the model-derived density reference is necessary because of the slow drift of the simulated density

away from the initial conditions during the integration.

Density is a natural coordinate for referencing the nitrate field in this investigation, as the eddy-induced nutrient transport mechanism of interest here is a result of vertical isopycnal displacements. The underlying assumption of this model is that the nitrate–density relationship below the euphotic zone is restored on time scales comparable to or shorter than the interval between vertical displacements associated with the supply events. Let us examine this assumption by considering a fluid parcel caught in an upwelling event. As the parcel rises into the euphotic zone, nitrate is removed by photosynthesis. As the parcel is subsequently downwelled into the aphotic zone, it is re-fortified with nutrients. Thus, it will bring new nitrate with it the next time it is upwelled. If the period of the vertical displacements were fast compared to the time scale for restoring the nitrate–density relationship, such a model would tend to overpredict the upward flux of nutrients. However, such does not appear to be the case. Because the bulk of the nutrient transport associated with mesoscale eddies is associated with upwelling in their interiors during eddy formation and intensification, the time scale most relevant to such nutrient injections is that of an eddy lifetime (McGillicuddy and Robinson, 1997). Typical mid-ocean eddies last for six months, with some Lagrangian drifter observations suggesting persistence of individual features for up to 430 days (see review by Richardson, 1993). Given that an upwelled fluid parcel will be, statistically speaking, downwelled in the next dynamical event in which it participates, it can be argued that the nominal period of vertical displacements is on the order of a year.

Estimation of the time scale for restoring the nitrate–density relationship is difficult because the underlying processes are not well understood. Several investigators have computed remineralization rates from seasonal variations in biogeochemical tracers, such as apparent oxygen utilization (*e.g.* Jenkins and Goldman, 1985; Sarmiento *et al.*, 1990) and the com-

bined inventories of oxygen, dissolved inorganic carbon, and nitrate (e.g. Ono *et al.*, 2000). Generally speaking, these studies indicate aphotic zone remineralization which is, on an annual basis, roughly consistent with organic matter production within the euphotic zone. Typically such calculations are based on mean seasonal variations which have been smoothed in some way to remove higher frequency variations. They yield estimates of remineralization necessary to maintain the observed seasonal cycles under the assumption of steady state. Thus such assessments provide an upper bound (order one year) on the time scale over which mesoscale perturbations to the nutrient distribution are restored.

There are at least three mechanisms by which the nitrate–density relationship might be restored following an eddy-driven productivity event. First, the nitrate deficit on a previously illuminated density surface could be restored by the remineralization of sinking particulate material from above. Clearly that sinking flux would not necessarily have originated from the eddy-upwelling event itself, for most of that material will have either already sunk or perhaps been downwelled as the previously uplifted density surface subsides. Thus this mechanism would rely primarily on the ambient flux of sinking particles. An estimate for the time scale of such remineralization could come from the sinking rate and the vertical distance between the strata of particulate formation and the density surface with the nitrate deficit. Using sinking rates of 1-10 m d^{-1} and eddy-driven isopycnal displacements on the order of 100m yields time scales of between 10 and 100 days.

[SCD to look into the issues of sinking/remineralization further.]

Alternatively, mesoscale patches of nitrate deficit could be restored via isopycnal mixing processes. Estimates of lateral diffusivity (which we equate with isopycnal diffusivity for the purposes of this discussion) in the open vary widely, and appear to be highly scale-dependent. In the analysis of the spread of a deliberately released tracer in the eastern North Atlantic,

Ledwell *et al.* (1998) documented lateral diffusivity of 0.07 m^2 s^{-1} operating on scales of 0.1 to 1km; 2 m^2 s^{-1} on scales of 1 to 10km, and on the order of 1000 m^2 s^{-1} for scales of 30 to 300 km. These estimates are roughly consistent with the scale dependence documented by Okubo (1971). A recent review of diffusivity estimates on basin scales in the North Atlantic by Robbins *et al.* (2000) (see their Table 1) reports values generally on the order of 1000 m^2 s^{-1}, essentially equivalent to Ledwell *et al.*'s estimate for the largest scales resolved in their study. A restoring time scale τ for this process can be estimated using $\tau \sim \frac{L^2}{K_H}$, where K_H is the lateral diffusivity and L is a length scale. With an eddy radius of 50km, the time scale for restoring mesoscale perturbations in the nutrient distribution vary widely with the diffusivity (Table 3). Use of the highest values of K_H represents an extreme upper bound, the eddies themselves are likely to be responsible for mixing at such large scales. Values in the range of 50-500 m^2 s^{-1} are probably more appropriate, yielding time scales that range from two months to two years. If the time scale for this process is two years, it becomes irrelevant. In contrast, a time scale of two months would not only be sufficient for restoring perturbations, but also constitute a pathway for additional nutrient supply during an isopycnal uplifting event.

Lastly, diapycnal processes can potentially contribute to restoration of the nutrient–density relationship, albeit on very long time scales. Estimates of the vertical diffusivity K_v (similarly taken to be equivalent to diapycnal diffusivity for the purposes of this discussion) from tracer release experiments suggest slow rates of mixing in the pycnocline (e.g. Ledwell *et al.*, 1993; Ledwell *et al.*, 1998). Using their canonical value of $K_v = 10^{-5}$ m^2 s^{-1} yields a time scale of order 10^4 days for new nitrate to penetrate vertically over a 100m interval of nutrient depletion created by an eddy-driven nutrient injection event. Clearly this is far longer than the yearly interval during which wintertime convection can temporarily mix down below

the depth of the deepest isopycnals that can be illuminated in a subsequent eddy upwelling event. Thus the annual period appears to be the shortest time scale on which diapycnal processes become relevant to this problem– and such will only be the case in regions where wintertime convection penetrates beyond the euphotic zone. In more permanently stratified areas the time scale will be much longer.

In summary, these three mechanisms offer a wide variety of time scales for replenishment of nutrient-depleted isopycnals, which range from as short as ten days to as long as a year. Given this uncertainty which stems from a lack of understanding of the processes at work, the best strategy from a modeling point of view is to carry out sensitivity analysis of the results with respect to variations of the nutrient restoring parameter. This will be discussed further below.

Advection numerics

The technical details of advection require special attention for biologically reactive tracers, owing to two characteristics which can sometimes set them apart from typical physical tracers. First, biological tracers often vary by orders of magnitude over short spatial scales, making regions of such high gradients prone to significant overshoot/undershoot (dispersion) problems associated with centered-time centered-space algorithms. This issue can become particularly troublesome due to the positive-definite nature of such tracers– even the slightest negative concentrations cause numerical instability in the equations governing biological dynamics.

A variety of different advection schemes have been used in recent intercomparison studies (Hecht *et al.*, 1998; Shchepetkin and McWilliams, 1998; Hasumi and Suginohara, 1999; Griffies *et al.*, 2000). Oschlies and Garcon (1999) compared two positive-definite schemes for tracer advection in their basin-scale biogeochemical model: first-order upwind differenc-

ing (also used by Sarmiento *et al.*, 1993) and the multidimensional positive definite central differences (MPDCD) of Lafore *et al.* (1998). Results of their biogeochemical model were sensitive to the numerical diffusion implicit in the upwind scheme. Such diffusion is significantly reduced in the MPDCD algorithm. On the basis of the Oschlies and Garcon results, we chose to use MPDCD. Basically, it is a standard centered difference advection scheme with a limit condition placed on the fluxes. The flux limitation ensures that advection cannot remove more scalar than is present at any given time step. This is accomplished by multiplying all fluxes going out of a cell by the factor

$$\min(1.0, \quad VC^{t-\Delta t}/(2\Delta t \Sigma F_i^{out} A_i))$$

where V is volume, C is concentration, t is time, Δt is timestep, F_i^{out} is an outward flux, and A_i is area of a grid cell face. The factor of 2 appears because the leapfrog timestepping then uses the fluxes to compute $C^{t+\Delta t}$. Thus the MPDCD scheme is a simple scaling factor applied to fluxes which is only different from 1.0 if the fluxes would drive the concentration negative. Fortunately, the additional computational cost of this procedure is minor (approximately 10%) and its implementation is straightforward.

Results

Mesoscale processes clearly impact new production throughout the basin (Figure 1, right panel; also see `http://science.whoi.edu/users/mcgillic/pop-bgc/pop-bgc.html` for animated presentation of these results). This instantaneous snapshot of the simulated biological uptake term is replete with mesoscale structure in nearly all areas except for the subpolar region where production is still strongly light-limited in mid-June. A zoom view of the solution near the BATS site reveals the detailed relationships between the mesoscale eddy field and nitrate (Figure 2). Although there is some enhancement of nitrate associated with

the frontal features inbetween eddies, the strongest anomalies are in the interiors of the eddy features. This phenomenology is consistent with regional model studies of McGillicuddy and Robinson (1997) and the conceptual model described above.

The coupled physical-biogeochemical model is run for a total of four years (January 1992 through December 1995). Discarding the first year because of the adjustment in the nitrate field that takes place during that time, the final three years of the simulation are used to compute a basin-scale map of annual new production (Figure 3). As expected, simulated new production is highest in the northern latitudes and in upwelling regions near the equator and off the coast of Africa. Generally speaking, magnitudes fall within the range of values estimated at several sites around the basin (Table 4).

Time series of the balance of terms at each site reveal the relative contributions of the various transprt terms fueling the simulated new production (Figure 4). Convection plays a significant role at the three northenmost sites. Both OWSI and NABE exhibit characteristics of the classical Sverdrup spring bloom: convective transport of nutrients into the surface layers during winter, followed by their removal during sprintime stratification. Latitudnal differences between these two sites are clearly evident; convection occurs earlier and the bloom occurs later at OWSI than it does at NABE. The relationship between convection and new production at BATS is quite different, where and "entrainment bloom" occurs. Nutrient input leads to a nearly simultaneous increase in new production because light is sufficient for rapid utlization. This type of bloom is characteristic of highly oligotrophic waters that are subject to wintertime convection. In contrast, convection plays no role in the permanently stratified waters at EUMELI. Its simulated annual new production of 0.10 ± 0.01 is sustained by an equipartition of fluxes between vertical diffusion and vertical advection (Table 5). The vertical diffusive flux is always positive and its temporal variations

are slow; vertical advection fluctuates much more rapidly, and is almost always positive. [check the variances in Table 5]. Horizontal advection does not yield a net contribution to the nutrient budget, although the term does reach relatively high values in association with intermittent pulses of vertical advection [look at movie for May-Dec 1994].

[mean and eddying components of vadv, hadv]

Discussion

To summarize, three different models suggest three different scenarios for nutrient supply to the euphotic zone of the subtropical gyre. The coarse-resolution simulations of Sarmiento *et al.* (1993) and Fasham *et al.* (1993) suggest the primary source of nitrate is through horizontal advection; in the eddy-permitting case of Oschlies *et al.* (2000) it is vertical mixing; in the present eddy-resolving case, eddy-driven vertical fluxes are sufficient to overcome mean wind-forced downwelling to make vertical advection a net source of nitrate. How can these different views of the nitrogen cycle be reconciled?

Although differences in the biogeochemical formulations of the three models cannot be dismissed, the fact that nitrate supply to the upper ocean is a physically-driven process points toward more detailed scrutiny of the differences in physical frameworks used to drive the simulations. For example, the large horizontal flux of nitrogen into the Sargasso Sea in the Sarmiento *et al.* (1993) and Fasham *et al.* (1993) simulations may be related to the impact of the horizontal mixing parameterization used at this relatively coarse resolution. In a careful analysis of the heat transport in GCMs, Böning *et al.* (1995) documented the presence of strong upwelling inshore of the Gulf Stream which significantly impacts structure of the simulated thermohaline circulation. The underlying causes of this aspect of the numerical solutions relate to the behavior of the mixing parameterization (which is typically applied on level surfaces in z-coordinate models) in the presence of strongly sloping isopycnals, as in

the western boundary current. This problem can be controlled to some degree by increased resolution and commensurate decrease in the coefficients of horizontal diffusion. This may explain the much reduced role of horizontal nitrate transport in the Oschlies *et al.* (2000) eddy permitting simulation and the eddy-resolving case described herein (Table 1).

Conclusions

Acknowledgments

We gratefully acknowledge the support of JPL, NASA and NSF. This is WHOI contribution number XXXXX.

Correspondence and requests for materials to D.J. McGillicuddy, Jr.

References

[1] D. Antoine, J.-M. Andre, and A. Morel, *Oceanic primary production 2. Estimation at global scale from satellite (Coastal Zone Color Scanner) chlorophyll*, Global Biogeochemical Cycles, 10 (1996), pp. 57–70.

[2] R. Armstrong, J. Sarmiento, and R. Slater, *Monitoring ocean productivity by assimilating satellite chlorophyll into ecosystem models*, in Ecological Time Series, New York, 1995, Chapman and Hall. T.M. Powell and J.H. Steele, eds.

[3] Y. Balkanski, P. Monfray, M. Battle, and M. Heimann, *Ocean primary production derived from satellite data: An evaluation with atmospheric oxygen measurements*, Global Biogeochemical Cycles, 13 (1999), pp. 257–271.

[4] B. Barnier, L. Siefridt, and P. Marchesiello, *Thermal forcing for a global ocean circulation model using a three-year climatology of ECMWF analyses*, Journal of Marine Systems, 6 (1995), pp. 363–380.

[5] M. Behrenfeld and P. Falkowski, *Photosynthetic rates derived from satellite-based chlorophyll concentration*, Limnol. Oceanogr., 42 (1997), pp. 1–20.

[6] C. Boning, W. Holland, F. Bryan, G. Danabasoglu, and J. McWilliams, *An overlooked problem in model simulation of the thermohaline circulation and heat transport in the Atlantic ocean*, Journal of Climate, 8 (1995), pp. 515–523.

[7] K. Bryan, *A numerical method for the study of the circulation of the world ocean*, J. Comp. Phys., (1969), pp. 347–376.

[8] K. Buesseler, *The de-coupling of production and particulate export in the surface ocean*, Global Biogeochemical Cycles, 12 (1998), pp. 297–310.

[9] J. Campbell and T. Aarup, *New production in the North Atlantic derived from seasonal patterns of surface chlorophyll*, Deep-Sea Research, 39 (1992), pp. 1669–1694.

[10] D. Capone, J. Zehr, H. Pearl, B. Bergman, and E. Carpenter, *Trichodesmium, a globally significant marine cyanobacterium*, Science, 276 (1997), pp. 1221–1229.

[11] I. Dadou, V. Garcon, V. Andersen, G. Flierl, and C. Davis, *Impact of the North Equatorial Current meandering ona pelagic ecosystem: a modelling approach*, J. Mar. Res., 54 (1996), pp. 311–342.

[12] S. Dutkiewicz, M. Follows, J. Marshall, and W. Gregg, *Interannual variability of phytoplankton abundances in the North Atlantic.* In press.

[13] R. Eppley, *Temperature and phytoplankton growth in the sea*, Fishery Bulletin, 17 (1972), pp. 15–24.

[14] P. Falkowski, D. Ziemann, Z. Kolber, and P. Bienfang, *Role of eddy pumping in enhancing primary production in the ocean*, Nature, 352 (1991), pp. 55–58.

[15] M. Fasham, H. Ducklow, and S. McKelvie, *A nitrogen-based model of plankton dynamics in the oceanic mixed layer*, J. Mar. Res., 48 (1990), pp. 591–639.

[16] M. Fasham, T. Platt, B. Irwin, and K. Jones, *Factors affecting the spatial pattern of the deep chlorophyll maximum in the region of the Azores Front*, Progress in Oceanography, 14 (1985), pp. 129–165.

[17] M. Fasham, J. Sarmiento, R. Slater, H. Ducklow, and R. Williams, *Ecosystem behavior at Bermuda Station "S" and Ocean Weather Station India: A general circulation model and observational analysis*, Global Biogeochemical Cycles, 7 (1993), pp. 379–415.

[18] G. Flierl and C. Davis, *Biological effects of Gulf Stream meandering*, J. Mar. Res., 51 (1993), pp. 529–560.

[19] P. Franks, J. Wroblewski, and G. Flierl, *Prediction of phytoplankton growth in response to the frictional decay of a warm-core ring*, J. Geophys. Res., 91 (1986), pp. 7603–7610.

[20] V. Garcon, A. Oschlies, S. Doney, D. McGillicuddy, and J. Waniek., *The role of mesoscale variability on plankton dynamics.* In press, Deep-Sea Research II.

[21] S. Griffies, R. Pacanowski, and R. Hallberg, *Spurious diapycnal mixing associated with advection in a z-coordinate ocean model*, Monthly Weather Review, 128 (2000), pp. 538–564.

[22] N. Gruber and J. Sarmiento, *Global patterns of marine nitrogen fixation and denitrification*, Global Biogeochemical Cycles, 11 (1997), pp. 235–266.

[23] H. Hasumi and N. Suginohara, *Sensitivity of a global ocean circulation model to tracer advection schemes*, Journal of Physical Oceanography, 29 (1999), pp. 2730–2740.

[24] M. Hecht, F. Bryan, and W. Holland, *A consideration of tracer advection schemes in a primitive equation ocean model*, J. Geophys. Res., 103 (1998), pp. 3301–3321.

[25] S. Hellerman and M. Rosenstein, *Normal monthly wind stress over the world ocean with error estimates*, Journal of Physical Oceanography, 13 (1983), pp. 1093–1104.

[26] R. Hood, A. Michaels, and D. Capone, *Answers sought to the enigma of marine nitrogen fixation*, EOS, 81 (2000), pp. 133,138–139.

[27] G. Hurtt and R. Armstrong, *A pelagic ecosystem model calibrated with BATS data*, Deep-Sea Research, 43 (1996), pp. 653–683.

[28] W. Jenkins, *Oxygen utilization rates in North Atlantic subtropical gyre and primary production in oligotrophic systems*, Nature, 300 (1982), pp. 246–248.

[29] ——, *Nitrate flux into the euphotic zone near Bermuda*, Nature, 331 (1988), pp. 521–523.

[30] ——, *The use of anthropogenic tritium and helium-3 to study subtropical gyre ventilation and circulation*, Phil. Trans. Roy. Soc., 325 (1988), pp. 43–61.

[31] ——, *Studying subtropical thermocline ventilation and circulation using tritium and ^3He*, J. Geophys. Res., 103 (1998), pp. 15,817–15,831.

[32] W. Jenkins and J. Goldman, *Seasonal oxygen cycling and primary production in the Sargasso Sea*, J. Mar. Res., 43 (1985), pp. 465–491.

[33] W. Jenkins and D. Wallace, *Tracer based inferences of new primary production in the sea*, in Primary Productivity and Biogeochemical Cycles in the Sea, P. Falkowski and A. Woodhead, eds., New York, 1992, Plenum Press, pp. 299–316.

[34] D. Kiefer and B. Mitchell, *A simple, steady-state description of phytoplankton growth based on absorbtion cross-section and quantum efficiency*, Limnol. Oceanogr., 28 (1983), pp. 770–776.

[35] J.-P. Lafore, J. Stein, N. Asencio, P. Bougeault, V. Ducrocq, J. Duron, C. Fischer, P. Hereil, P. Mascart, V. Masson, J. Pinty, J. Redelsperger, E. Richard, and J. V.-G. de Arellano, *The meso-NH atmospheric simulation system, I, Adiabatic formulation and control simulations*, Annales Geophysicae, 16 (1998), pp. 90–109.

[36] E. Laws, P. Falkowski, W. Smith, H. Ducklow, and J. McCarthy, *Temperature effects on export production in the open ocean*, Global Biogeochemical Cycles, (2000). Global Biogeochem. Cycles, in press.

[37] J. Ledwell, A. Watson, and C. Law, *Evidence for slow mixing across the pycnocline from an open-ocean tracer-release experiment*, Nature, 364 (1993), pp. 701–703.

[38] ——, *Mixing of a tracer released in the pycnocline*, 1998.

[39] S. Levitus, *Climatological atlas of the world ocean*, in NOAA Prof. Paper No. 13, U.S. Govt. Printing Office, Washington DC, 1982, p. 173pp.

[40] M. Lewis, W. Harrison, N. Oakley, D. Hebert, and T. Platt, *Vertical nitrate fluxes in the oligotrophic ocean*, Science, 234 (1986), pp. 870–873.

[41] J. Liebig, *On chemical processes in the nutrition of vegetables*, in Chemistry and its applications to agriculture and physiology, L. Playfair, Peterson, PA, 1845.

[42] F. Lipschultz and N. Owens, *An assessment of nitrogen fixation as a source of nitrogen to the North Atlantic Ocean*, Biogeochemistry, 35 (1996), pp. 261–274.

[43] A. Mahadevan and D. Archer, *Modeling the impact of fronts and mesoscale circulation on the nutrient supply and biogeochemistry of the upper ocean*, J. Geophys. Res., 105 (2000), pp. 1209–1225.

[44] J. Martin, S. Fitzwater, R. Gordon, C. Hunter, and S. Tanner, *Iron, primary production and carbon-nitrogen flux studies during the JGOFS North Atlantic Bloom Experiment*, Deep-Sea Research, 40 (1993), pp. 115–134.

[45] D. McGillicuddy, R. Johnson, D. Siegel, , A. Micheals, N. Bates, and A. Knap, *Mesoscale variations of biogeochemical properties in the Sargasso Sea*, J. Geophys. Res., 104 (1999), pp. 13,381–13,394.

[46] D. McGillicuddy, V. Kosnyrev, J. Ryan, and J. Yoder, *Covariation of mesoscale ocean color and sea surface temperature patterns in the Sargasso Sea*, 2000. In press, *Deep-Sea Research II*.

[47] D. McGillicuddy and A. Robinson, *Eddy induced nutrient supply and new production in the Sargasso Sea*, Deep-Sea Research, 44 (1997), pp. 1427–1449.

[48] D. McGillicuddy, A. Robinson, D. Siegel, H. Jannasch, R. Johnson, T. Dickey, J. McNeil, A. Michaels, and A. Knap, *Influence of mesoscale eddies on new production in the Sargasso Sea*, Nature, 394 (1998), pp. 263–265.

[49] J. McNeil, H. Jannasch, T. Dickey, D. McGillicuddy, M. Brzezinski, and C. Sakamoto, *New chemical, bio-optical and physical observations of upper ocean response to the passage of a mesoscale eddy off Bermuda*, J. Geophys. Res., 104 (1999), pp. 15,537–15,548.

[50] A. Michaels, A. Knap, R. Dow, K. Gundersen, R. Johnson, J. Sorenson, A. Close, G. Knauer, S. Lohrenz, V. Asper, M. Tuel, and R. Bidigare, *Seasonal patterns of ocean biogeochemistry at the U.S. JGOFS Bermuda Atlantic Time-series Study site*, Deep-Sea Research, 41 (1994), pp. 1013–1038.

[51] A. Michaels, D. Olson, J. Sarmiento, J. Ammerman, K. Fanning, R. Jahnke, A. Knap, F. Lipschultz, and J. Prospero, *Inputs, losses and transformations of nitrogen and phosphorus in the pelagic North Atlantic Ocean*, Biogeochemistry, 35 (1996), pp. 181–226.

[52] F. Morel, *Process studies in eutrophic, mesotrophic and oligotrophic regimes within the tropical northeast Atlantic*, in The changing carbon cycle, IGBP Book Ser., R. Hanson,

H. Ducklow, and J. Field, eds., Cambridge University Press, New York, 1999, pp. 338–374.

[53] A. Okubo, *Oceanic diffusion regimes*, Deep-Sea Research, 18 (1971), pp. 789–802.

[54] S. Ono, A. Ennyu, R. Najjar, and N. Bates, *Shallow remineralization in the Sargasso Sea estimated from seasonal variations in oxygen and dissolved inorganic carbon and nitrate*. In press, *Deep-Sea Research II*.

[55] A. Oschlies and V. Garcon, *Eddy-induced enhancement of primary production in a model of the North Atlantic Ocean*, Nature, 394 (1998), pp. 266–269.

[56] ——, *An eddy-permitting coupled physical-biological model of the North Atlantic 1. Sensitivity to advection numerics and mixed layer physics*, Global Biogeochemical Cycles, 13 (1999), pp. 135–160.

[57] A. Oschlies, W. Koeve, and V. Garcon, *An eddy-permitting coupled physical-biological model of the North Atlantic 2. Ecosystem dynamics and comparison with satellite and JGOFS local studies data*, Global Biogeochemical Cycles, 14 (2000), pp. 499–523.

[58] R. Pacanowski and S. Philander, *Parameterization of vertical mixing in numerical models of tropical oceans*, Journal of Physical Oceanography, 11 (1981), pp. 1443–1451.

[59] U. Passow and R. Peinert, *The role of plankton in particle flux: two case studies from the northeast Atlantic*, Deep-Sea Research II, 40 (1993), pp. 573–585.

[60] T. Platt, C. Gallegos, and W. Harrison, *Photoinhibition of photosynthesis in natural assemblages of marine phytoplankton*, J. Mar. Res., 38 (1980), pp. 687–701.

[61] P. Richardson, *A census of eddies observed in north atlantic SOFAR float data*, Progress in Oceanography, 31 (1993), pp. 1–50.

[62] P. Robbins, J. Price, W. Owens, and W. Jenkins, *The importance of lateral diffusion for the ventilation of the lower thermocline in the subtropical North Atlantic*, Journal of Physical Oceanography, 30 (2000), pp. 67–89.

[63] R. Sambrotto, J. Martin, W. Broenkow, C. Carlson, and S. Fitzwater, *Nitrate utilization in surface waters of the Iceland Basin during spring and summer of 1989*, Deep-Sea Research II, 40 (1993), pp. 441–457.

[64] J. Sarmiento, R. Slater, M. Fasham, H. Ducklow, J. Toggweilera, and G. Evans, *A seasonal three-dimensional ecosystem model of nitrogen cycling in the North Atlantic euphotic zone*, Global Biogeochemical Cycles, 7 (1993), pp. 417–450.

[65] J. Sarmiento, G. Thiele, R. Key, and W. Moore, *Oxygen and nitrate new production and remineralization in the North Atlantic subtropical gyre*, J. Geophys. Res., 95 (1990), pp. 18303–18315.

[66] E. Schulenberger and J. Reid, *The Pacific shallow oxygen maximum, deep chlorophyll maximum, and primary productivity, reconsidered*, Deep-Sea Research, 28A (1981), pp. 901–919.

[67] A. Shchepetkin and J. McWilliams, *Quasi-monotone advection schemes based on explicit locally adaptive dissipation*, Monthly Weather Review, 126 (1998), pp. 1541–1580.

[68] D. Siegel, D. McGillicuddy, and E. Fields, *Mesoscale eddies, satellite altimetry and new production in the Sargasso Sea*, J. Geophys. Res., 104 (1999), pp. 13,359–13,379.

[69] R. Slater, J. Sarmiento, and M. Fasham, *Some parametric and structural simulations with a three-dimensional ecosystem model of nitrogen cycling in the North Atlantic euphotic zone*, in Towards a model of ocean biogeochemical processes, Berlin, 1993, Springer-Verlag. G.T. Evans and M.J.R. Fasham, eds.

[70] C. Smith, K. Richards, and M. Fasham, *The impact of mesoscale eddies on plankton dynamics in the upper ocean*, Deep-Sea Research, 43 (1996), pp. 1807–1832.

[71] R. Smith, J. Dukowicz, and R. Malone, *Parallel ocean circulation modeling*, Physica D, 60 (1992), pp. 38–61.

[72] R. Smith, M. Maltrud, F. Bryan, and M. Hecht, *Numerical simulation of the North Atlantic Ocean at 1/10°*, Journal of Physical Oceanography, 30 (2000), pp. 1532–1561.

[73] S. Spall and K. Richards, *A numerical model of mesoscale frontal instabilities and plankton dynamics– I. Model formulation and initial experiments*, Deep-Sea Research I, 47 (2000), pp. 1261–1301.

[74] W. Spitzer and W. Jenkins, *Rates of vertical mixing, gas exchange and new production: estimates from seasonal gas cycles in the upper ocean near Bermuda*, J. Mar. Res., 47 (1989), pp. 169–196.

[75] V. Strass, *Chlorophyll patchiness caused by mesoscale upwelling at fronts*, Deep-Sea Research, 39 (1992), pp. 75–96.

[76] V. Strass and J. Woods, *New produciton in the summer revealed by the meridional slope of the deep chlorophyll maximum*, Deep-Sea Research, 38 (1991), pp. 35–56.

[77] R. Williams and M. Follows, *The Ekman transfer of nutrients and maintenance of new production over the North Atlantic*, Deep-Sea Research, 45 (1997), pp. 461–489.

[78] J. Woods, *Mesoscale upwelling and primary production*, in Toward a Theory on Biological-Physical Interactions in the World Ocean, B. Rothschild, ed., Dordrecht, 1988, D. Reidel.

Figure 1: Snapshots of temperature and new production in a 0.1° simulation of the North Atlantic. The Sargasso Sea subdomain for Figure 2 is indicated.

Figure 2: Snapshots of potential density and nitrate extracted from the Sargasso Sea subdomain shown in Figure 1.

Figure 3: Annual new production ($\log_{10}$ mol N m^{-2} yr^{-1}) averaged over the final year of a two year simulation. Note that production on continental shelves (<100m) is not realistic due to the simplicity of the biological model.

Figure 4: Term balances for nutrient cycling at selected sites throughout the basin: new production (bold solid), convection (thin solid), vertical diffusion (thin dashed), vertical advection (bold dashed) and horizontal advection plus diffusion (dotted).

	Fasham *et al.* (1993) 2.0° (coarse res.)	Oschlies *et al.* (2000) 0.3° (eddy permitting)	This study 0.1° (eddy resolving)
Horizontal transport	0.38	0.10	0.08 ± 0.06
Vertical advection	-0.16	-0.13	0.09 ± 0.04
Vertical mixing	0.35	0.66	0.50 ± 0.05
convection	0.34	–	0.39 ± 0.04
diffusion	0.01	–	0.11 ± 0.01
Annual New Production	0.57	0.63	0.67 ± 0.06

Table 1: Nitrate budgets and annual new production (both in mol N m^{-2} yr^{-1}) at the BATS site in three different models. Note that Oschlies *et al.* (2000) do not distinguish between convection and diffusion in the vertical mixing term. Geochemical estimates in this region suggest an annual new production of 0.50 ± 0.14 mol N m^{-2} yr^{-1} (Table 4).

μ_0	maximum new production rate	0.5 mmol N m^{-3} d^{-1}
k_n	half-saturation constant for nitrate limitation	0.1 mmol N m^{-3}
α	initial slope of light response	0.05 m^2 W^{-1}
τ	nitrate restoring time scale	0.1 d^{-1}

Table 2: Parameters of the nutrient transport model.

K_H (m^2 s^{-1})	τ (days)
1000	29
500	58
100	289
50	578
10	2894

Table 3: Estimated time scale τ for restoring the nutrient–density relationship as a function of lateral diffusivity K_H.

Site	Annual New Production		Method	Reference
	Simulated	Observed		
BATS		0.45 ± 0.10	O_2 utilization	Jenkins and Wallace (1992)
(32N,64W)		0.42 ± 0.09		Jenkins and Goldman (1985)
		0.46 ± 0.09	O_2 production	Jenkins and Goldman (1985)
		0.39 ± 0.16		Spitzer and Jenkins (1989)
		0.51 ± 0.14		Spitzer and Jenkins (1989)
		0.56 ± 0.16	He flux gauge	Jenkins (1988a)
		0.47 ± 0.15		Jenkins (pers. comm.)
		0.70 ± 0.20		Jenkins (1998)
	0.67 ± 0.06	0.39 – 0.70		
NABE		0.90 ± 0.30	PP and O_2 data	Balkanski *et al.* (1999)
(47N,20W)		1.26 ± 0.63	PP and f-ratio	Behrenfeld and Falkowski (1997)
				Buesseler (1998)
				Martin *et al.* (1993)
		0.82 ± 0.44	PP and f-ratio	Antoine *et al.* (1996)
				Buesseler (1998)
				Martin *et al.* (1993)
		2.52 ± 0.63	SeaWiFS and model	Laws *et al.* (2000)
		0.69	seasonal Chl and NO_3	Campbell and Aarup (1992)
		0.43	seasonal Chl and NO_3	Strass and Woods (1991)
	1.45 ± 0.07	0.43 – 2.52		
OWS I		0.90 ± 0.30	PP and O_2 data	Balkanski *et al.* (1999)
(59N,19W)		0.80	Apr-Aug NO_3 util.	Sambrotto *et al.* (1993)
		1.92 ± 0.35	PP and f-ratio	Behrenfeld and Falkowski (1997)
				Sambrotto *et al.* (1993)
				Fasham *et al.* (1993)
		0.79 ± 0.16	PP and f-ratio	Antoine *et al.* (1996)
				Sambrotto *et al.* (1993)
				Fasham *et al.* (1993)
		2.52 ± 0.63	SeaWiFS and model	Laws *et al.* (2000)
		0.53	seasonal Chl and NO_3	Campbell and Aarup (1992)
	1.46 ± 0.03	0.53 – 2.52		
EUMELI		0.45 ± 0.15	PP and O_2 data	Balkanski *et al.* (1999)
(21N,31W)		0.19 ± 0.16	PP and $\delta^{15}N$ uptake	Morel (1999)
		0.14 ± 0.08	PP and f-ratio	Behrenfeld and Falkowski (1997)
				Morel (1999)
		0.16 ± 0.07	PP and f-ratio	Antoine *et al.* (1996)
				Morel (1999)
		0.10	seasonal Chl and NO_3	Campbell and Aarup (1992)
		0.02	sediment traps	Passow and Peinert (1993)
	0.10 ± 0.01	0.02 – 0.45		

Table 4: Annual new production in the North Atlantic (mol N m^{-2} yr^{-1}). Simulated values are compared with the range of observational estimates in the final entry for each site. Note that the standard deviation reported for the simulated values reflects interannual variability in yearly means.

	BATS	NABE	OWS I	EUMELI
Horizontal transport	0.08 ± 0.06	0.30 ± 0.09	-0.18 ± 0.34	0.00 ± 0.01
advection	0.08 ± 0.06	0.31 ± 0.09	-0.18 ± 0.34	0.00 ± 0.01
diffusion	0.00 ± 0.00	0.00 ± 0.00	0.00 ± 0.00	0.00 ± 0.00
Vertical mixing	0.50 ± 0.05	1.31 ± 0.25	1.75 ± 0.12	0.05 ± 0.01
convection	0.39 ± 0.04	1.01 ± 0.20	1.37 ± 0.09	0.00 ± 0.00
diffusion	0.11 ± 0.01	0.30 ± 0.06	0.38 ± 0.03	0.05 ± 0.01
Vertical advection	0.09 ± 0.04	-0.15 ± 0.03	-0.15 ± 0.22	0.05 ± 0.01
Annual New Production	0.67 ± 0.06	1.45 ± 0.07	1.46 ± 0.03	0.10 ± 0.01

Table 5: Simulated nitrate budgets and annual new production (mol N m^{-2} yr^{-1}) at four different sites in the North Atlantic. Standard deviations are computed from yearly means and thus reflect interannual variability only.

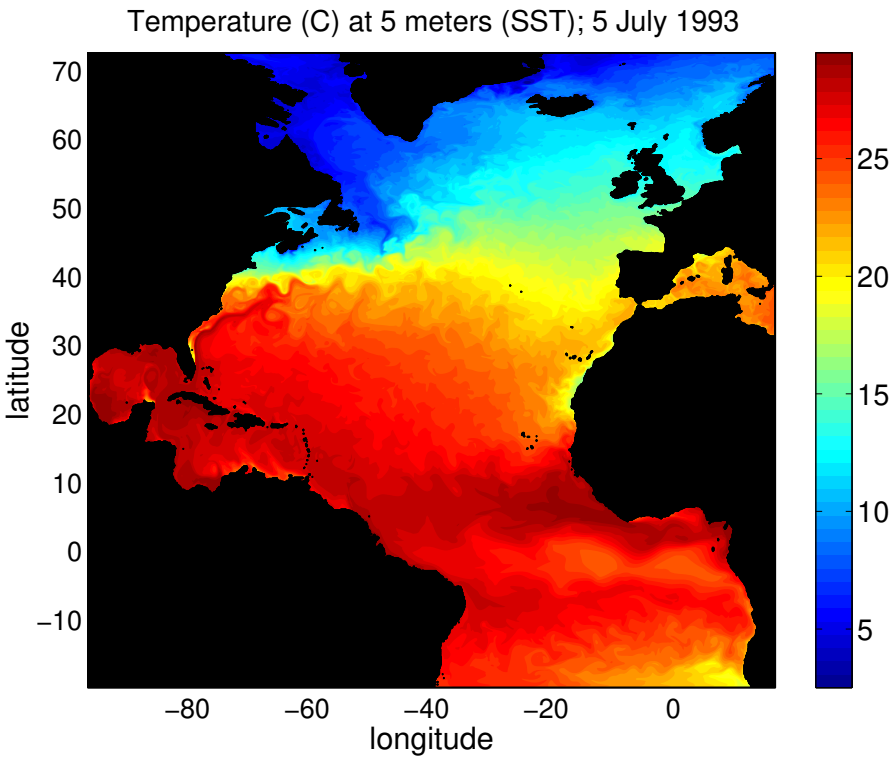
Temperature (C) at 5 meters (SST); 5 July 1993
70
60
50
40
30
20
10
0
−10
latitude
−80
−60
−40
−20
0
longitude
25
20
15
10
5

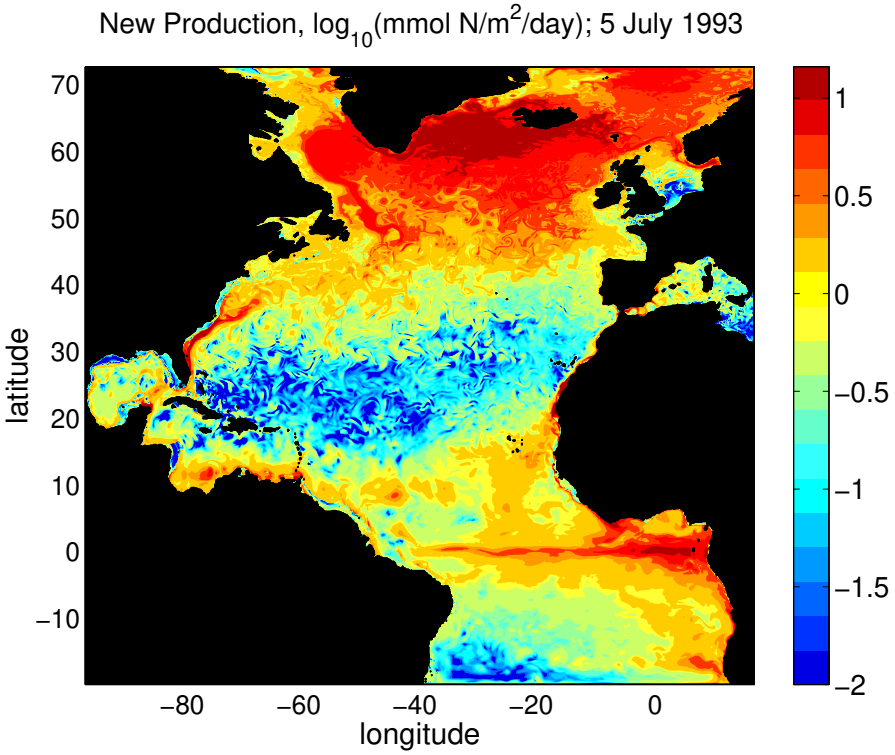
New Production, log10(mmol N/m2/day); 5 July 1993
70
60
50
40
30
20
10
0
−10
latitude
−80
−60
−40
−20
0
longitude
1
0.5
0
−0.5
−1
−1.5
−2

Figure 1.

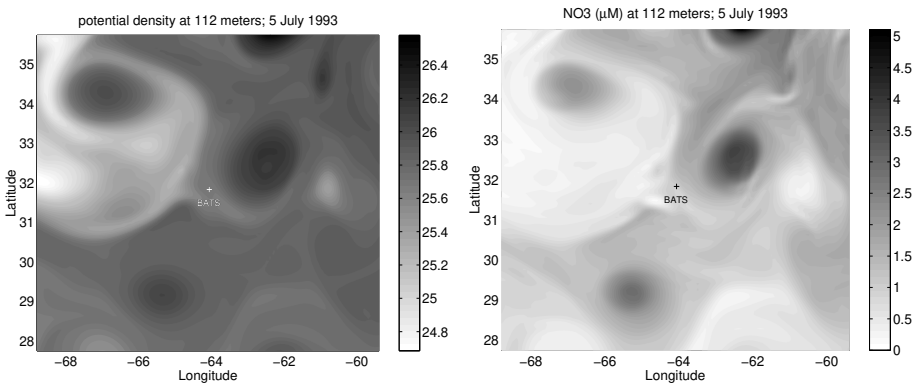
potential density at 112 meters; 5 July 1993
Latitude
Longitude
BATS
35
34
33
32
31
30
29
28
−68
−66
−64
−62
−60
26.4
26.2
26
25.8
25.6
25.4
25.2
25
24.8
NO3 (μM) at 112 meters; 5 July 1993
Latitude
Longitude
BATS
5
4.5
4
3.5
3
2.5
2
1.5
1
0.5
0

Figure 2.

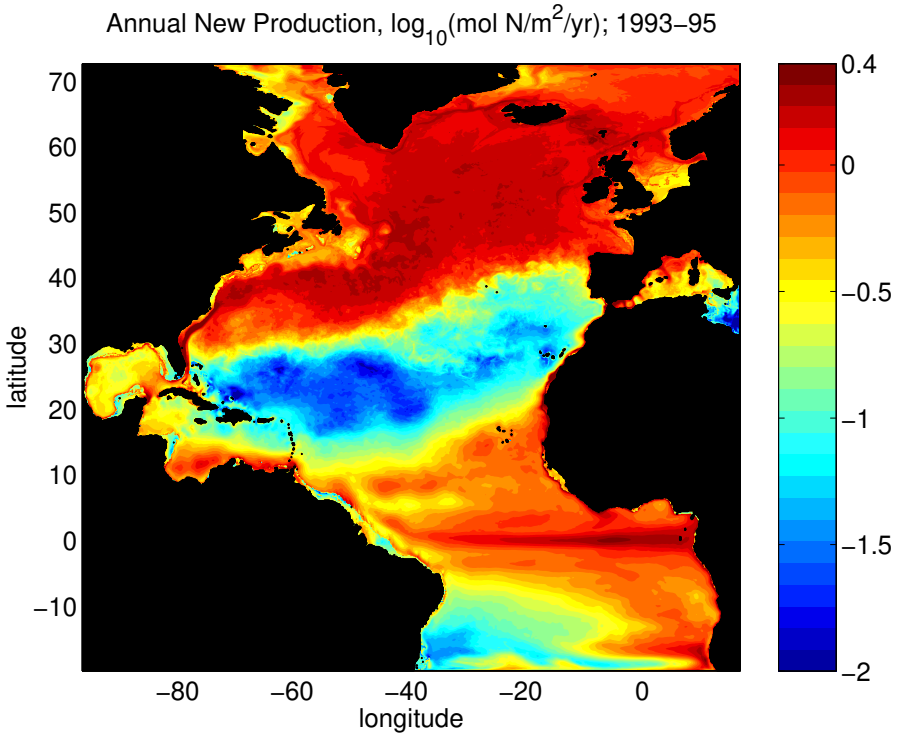
Annual New Production, log10(mol N/m2/yr); 1993–95
70
60
50
40
30
20
10
0
−10
latitude
−80
−60
−40
−20
0
longitude
0.4
0
−0.5
−1
−1.5
−2

Figure 3.

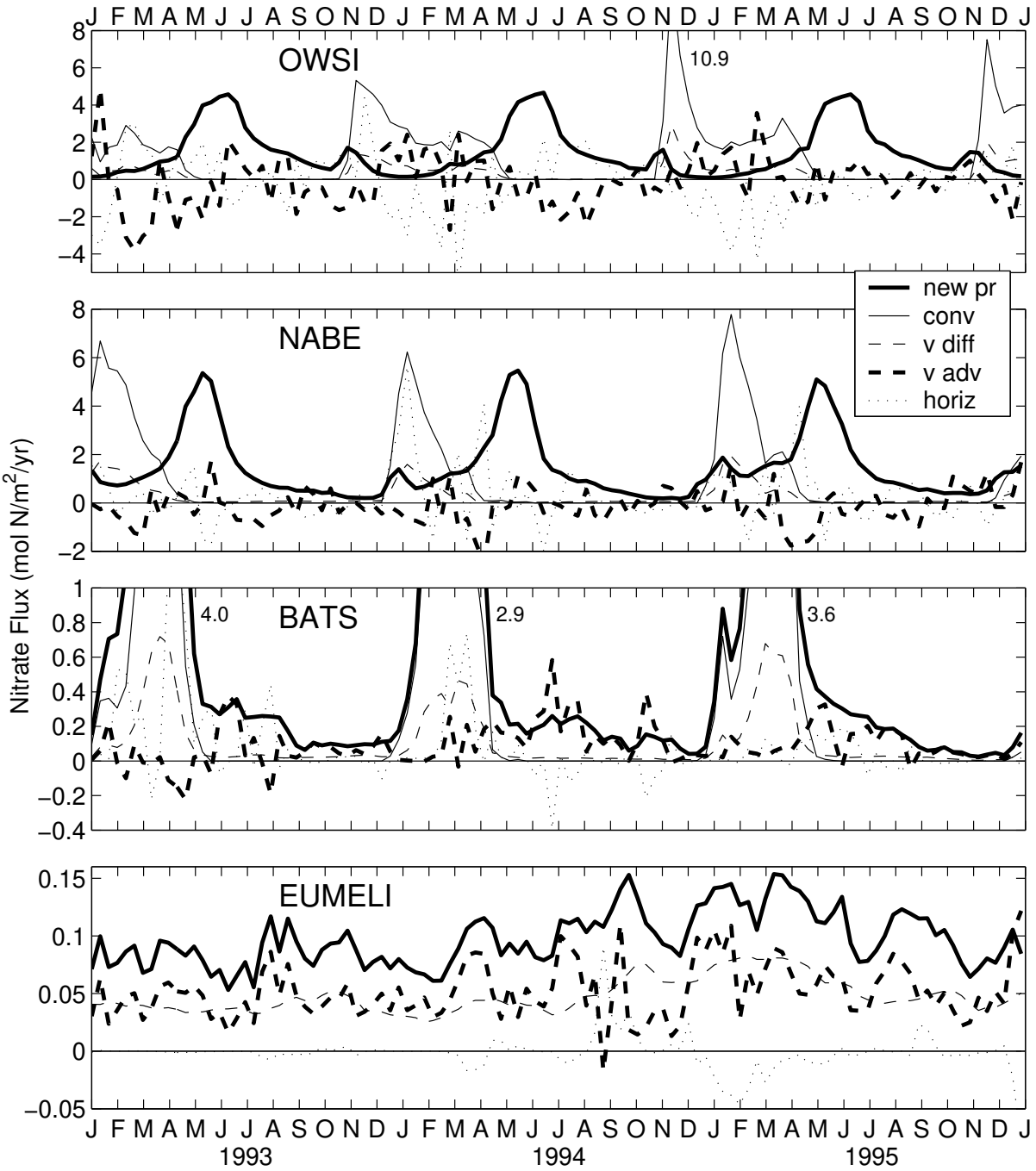
J F M A M J J A S O N D J F M A M J J A S O N D J F M A M J J A S O N D J
OWSI
10.9
NABE
new pr
conv
v diff
v adv
horiz
BATS
4.0
2.9
3.6
EUMELI
Nitrate Flux (mol N/m^2/yr)
1993
1994
1995

Figure 4.